

## Ordering of interstitial oxygen atoms in $\text{La}_2\text{NiO}_{4+\delta}$ observed by transmission electron microscopy

Zenji Hiroi, Takeshi Obata, Mikio Takano, and Yoshichika Bando  
*Institute for Chemical Research, Kyoto University, Uji, Kyoto-fu 611, Japan*

Yasuo Takeda and Osamu Yamamoto  
*Faculty of Engineering, Mie University, Tsu 514, Japan*  
 (Received 20 March 1990)

Structural properties of  $\text{La}_2\text{NiO}_{4+\delta}$  have been investigated by electron diffraction and transmission electron microscopy. Two types of homologous series of superstructures have been found for samples containing excess oxygen, i.e.,  $\delta > 0$ . They are  $2a \times ka \times lc$  ( $k, l = n$  or  $2n$  depending upon  $n$ ; the most frequently observed sets are  $k/2 = l/2 = n = 2$  and  $k = l/2 = n = 3$ ) and  $\sqrt{2}a \times p\sqrt{2}a \times qc$  (most frequently  $p = 2$  and  $q = 1$ ), where  $a \times a \times c$  stands for the  $\text{K}_2\text{NiF}_4$ -type cell. The origin of these superstructures has been assigned to the ordering of excess oxygen atoms located interstitially between two adjacent LaO layers. The most probable ordering schemes are proposed. Phases with discrete oxygen contents of  $\text{La}_2\text{NiO}_{4+\delta}$  with  $\delta = 0, \dots, \frac{1}{8}, \frac{1}{6}, \frac{1}{4}$  seem to exist.

Oxygen nonstoichiometry and its influences on structural and physical properties of  $\text{La}_2\text{MO}_{4+\delta}$  ( $M = \text{Cu}, \text{Ni}, \text{Co}$ ) have recently been studied extensively. Interest in these compounds has been renewed by a finding that excess oxygen atoms inject holes into  $\text{CuO}_2$  sheets of the  $M = \text{Cu}$  compound and render it superconducting.<sup>1</sup> According to powder and single-crystal neutron-diffraction studies,<sup>2,3</sup> the excess oxygen atoms are located between two adjacent LaO layers, at interstitial sites tetrahedrally coordinated by La atoms, and this leads to a serious distortion of the lattice around them. Moreover, it has been suggested that a miscibility gap exists in the temperature versus oxygen-content ( $4 + \delta$ ) phase diagram, which is  $0 < \delta < 0.08$  for  $\text{La}_2\text{CuO}_{4+\delta}$ ,  $0.02 < \delta < 0.12$  for  $\text{La}_2\text{NiO}_{4+\delta}$ , and  $0 < \delta < 0.15$  for  $\text{La}_2\text{CoO}_{4+\delta}$  at room temperature.<sup>1-5</sup>

In perovskites and related compounds showing oxygen nonstoichiometry, ordering of oxygen vacancies has long been an interesting topic of solid-state chemistry.<sup>6</sup> However, ordering of interstitial oxygen atoms has been relatively unknown. Very recently, the modulated structure found in superconducting oxides of the Bi-Sr-Ca-Cu-O system has been attributed to ordering of excess oxygen atoms in  $\text{BiO}_{1+\delta}$  sheets.<sup>7,8</sup> It is interesting to notice that there is a structural similarity between the Bi and the La systems: The BiO and LaO double layers of the NaCl type are sandwiched by perovskite-like layers which are  $\text{SrO}/\text{Ca}_{m-1}\text{Cu}_m\text{O}_{2m}/\text{SrO}$  in the former and  $\text{CuO}_2$  in the latter. The lattice mismatch between these two different types of layers must be the origin of the oxygen incorporation.<sup>9,10</sup> We have expected that the excess oxygen atoms in  $\text{La}_2\text{MO}_{4+\delta}$  also become ordered to minimize the increase in elastic energy caused by the incorporation. However, the previous diffraction studies did not find such ordering. We have examined  $\text{La}_2\text{NiO}_{4+\delta}$  with various oxygen contents by means of electron diffraction and transmission electron microscopy, because these methods also give information on ordered structures: If the order-

ing is short ranged or multiple in mode, these methods should be more advantageous in comparison with x-ray and neutron-diffraction methods which detect averaged structure. As a result, we have found two types of homologous series of superstructures. They can be described as  $2a \times ka \times lc$  and  $\sqrt{2}a \times p\sqrt{2}a \times qc$  on the basis of the ideal tetragonal  $\text{K}_2\text{NiF}_4$ -type structure. The most probable ordering models of interstitial oxygen atoms will be presented.

Samples were prepared by a usual ceramic method by firing mixtures of  $\text{La}_2\text{O}_3$  (prefired at  $900^\circ\text{C}$  to remove hydroxides and carbonates) and NiO at  $1100^\circ\text{C}$  repeatedly. The oxygen contents of  $\delta = 0.04, 0.07, 0.10,$  and  $0.12$  were varied by changing the temperature and atmosphere of subsequent annealing. A sample with  $\delta = 0.20$  was synthesized by annealing at  $600^\circ\text{C}$  under 600 atm oxygen pressure for 24 h. A stoichiometric sample of  $\delta = 0.0$  was prepared by reacting  $\text{La}_2\text{O}_3$  and NiO in a sealed quartz tube at  $1100^\circ\text{C}$  for 20 h, which had a light yellowish-brown color.<sup>2</sup> Oxidation made it black, which occurred even at room temperature in air. Certain samples were further annealed at  $200^\circ\text{C}$  for 48 h in sealed quartz tubes. The overall oxygen content was determined by means of iodometry. All the samples were examined by powder x-ray diffraction (XRD), electron diffraction (ED), and transmission electron microscopy.

A wide variety of superlattice reflections have been observed in ED patterns from various samples except  $\delta = 0$ , revealing that at least two homologous series of superstructures exist in nonstoichiometric  $\text{La}_2\text{NiO}_{4+\delta}$ . One of them is characterized by one-dimensional arrays of superlattice spots along the  $[011]^*$  direction with an interval of one- $n$ th of the  $[011]^*$  length. The  $n = 2$  and 3 patterns are shown in Fig. 1. Corresponding lattice images from thick crystals are shown in Fig. 2, where such bright (011) lattice fringes as marked with the arrows appear in every second place in Fig. 2(a) and in every third place in Fig. 2(b). These superstructures with small  $n$  values are

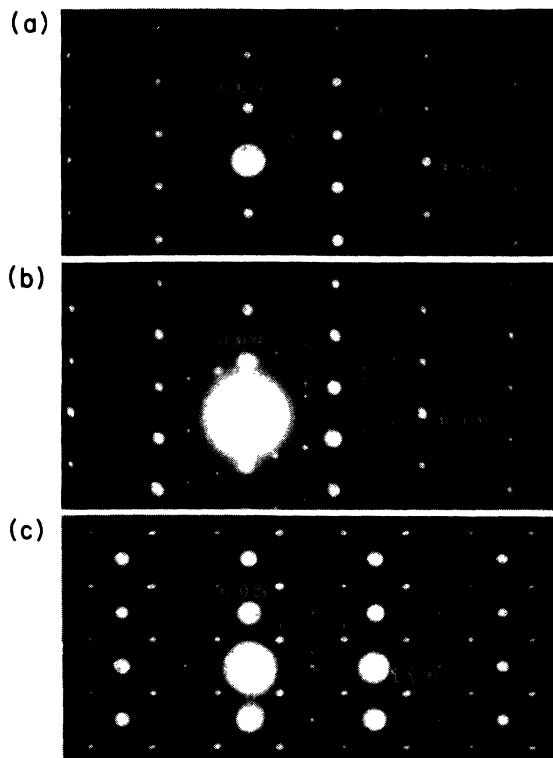


FIG. 1. [100] zone axis ED patterns of the  $2a \times ka \times lc$ -type superstructures with (a)  $k/2 = l/2 = n = 2$ , (b)  $k = l/2 = n = 3$ , and (c) the  $[1\bar{1}0]$  ED pattern from the  $\sqrt{2}a \times 2\sqrt{2}a \times c$  structure. Certain superlattice reflection spots are marked by arrows.

formed over relatively wide ranges of  $10^4$  nm<sup>2</sup>, while longer periodicities up to  $n = 12$  appear very locally. Examination of several zone axes ED patterns has revealed that this type of superstructure is described as  $2a \times ka \times lc$  ( $k, l = n$  or  $2n$  depending upon  $n$ ) on the basis of the ideal  $K_2NiF_4$ -type unit cell; for example,  $2a \times 4a \times 4c$  for  $n = 2$  and  $2a \times 3a \times 6c$  for  $n = 3$ .

Another type of superstructure is  $\sqrt{2}a \times p\sqrt{2}a \times qc$  as typically seen in the  $[1\bar{1}0]$  zone axis ED pattern of Fig. 1(c) and the lattice image of Fig. 3 for  $(p, q) = (2, 1)$ . Strong superlattice reflections marked with arrows in the ED pattern produce an interesting contrast variation along the  $[110]$  axis with a period of  $2\sqrt{2}a$ , and the variation changes its phase by  $\pi/2$  along the  $c$  axis. It should be noticed that the periodically modulated image pattern in Fig. 3 is rather similar to that of the modulation in the Bi compounds.<sup>9-11</sup> Incommensurate periodicities of  $2 < p < 3$  were also frequently observed, where two modes with  $p = 2$  and 3 are probably mixed very microscopically.

The origin of these superstructures is naturally attributed to ordering of the excess oxygen atoms: They were found only in samples with  $\delta > 0$ , and moreover, high-resolution lattice images, not shown here, have strongly suggested that the periodically arranged structural singular points which define their superlattice unit cell always lie within the LaO double layer containing excess oxygen.<sup>12</sup> The most probable structural models for the  $2a \times ka \times lc$  structures with  $k/2 = l/2 = n = 2$  and  $k = l/2$

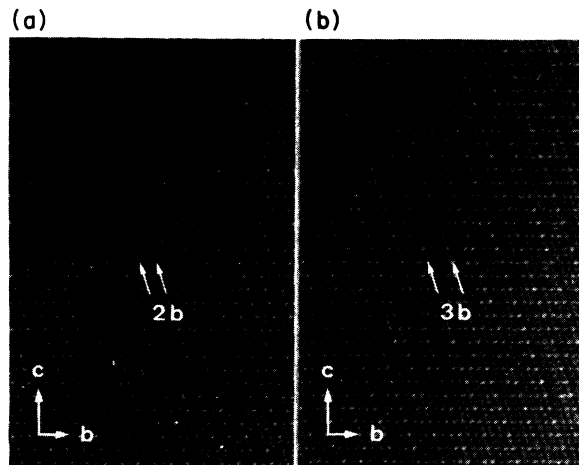


FIG. 2. Lattice images of the  $2a \times ka \times lc$ -type superstructures for (a)  $k/2 = l/2 = n = 2$  and (b)  $k = l/2 = n = 3$  corresponding to the ED patterns in Figs. 1(a) and 1(b), respectively. The brighter (011) lattice fringes are periodically seen as shown by arrows.

$n = 3$  that consistently explain the observed reciprocal lattices and the high-resolution images are depicted in Fig. 4. The interstitial oxygen atoms coordinated tetrahedrally by La atoms are aligned along the  $[1\bar{1}1]$  direction within a (011) plane. The rows are separated from each other by  $2a$  along the  $a$  axis. These special (011) planes are separated from each other by  $na$  along the  $b$  axis as shown in Figs. 4(b) and 4(c). In Fig. 4(b) these planes are further shifted from each other by  $a$  along the  $a$  axis. The resulting unit-cell size is  $2a \times 4a \times 4c$  in Fig. 4(b) and  $2a \times 3a \times 6c$  in Fig. 4(c) as experimentally found. These models give excess oxygen contents of  $1/2n$  for arbitrary  $n$ ; for example,  $\delta = 0.25$  for  $n = 2$  and

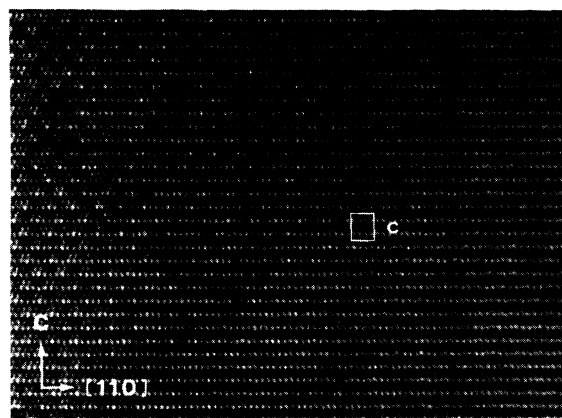


FIG. 3. Lattice images of the  $\sqrt{2}a \times 2\sqrt{2}a \times c$ -type superstructures corresponding to the ED pattern of Fig. 1(c). The fine contrast variation within the LaO layers due to the superlattice is clearly seen, which resembles that of the modulation found in the Bi compounds.

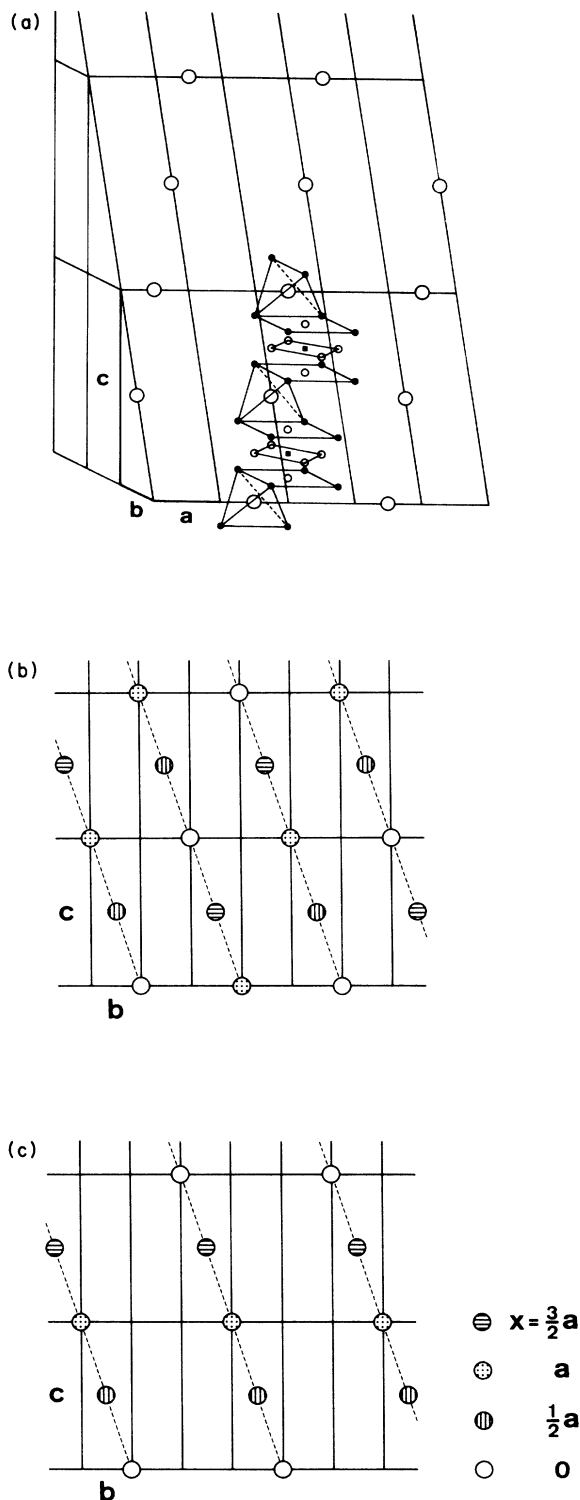


FIG. 4. Schematic representations of the most probable structure models for the  $2a \times ka \times lc$ -type superstructures in which interstitial oxygen atoms are ordered. Large and small open circles in (a) represent interstitial and normal oxygen atoms, respectively. Solid circles and squares indicate La and Cu atoms, respectively. Specific (011) planes containing interstitial oxygen atoms periodically appear as in (b) ( $n=2$ ) and (c) ( $n=3$ ). The resulting unit cell size is  $2a \times 4a \times 4c$  in (b) and  $2a \times 3a \times 6c$  in (c) as experimentally found.

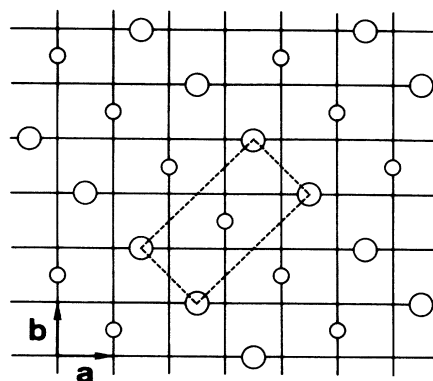


FIG. 5. Schematic illustration of the most probable basal-plane structure of the  $\sqrt{2}a \times 2\sqrt{2}a \times c$  superlattice. Large and small circles represent interstitial oxygen atoms at  $z=0$  and  $z=c/2$ , respectively.

$\delta=0.17$  for  $n=3$ . There can exist a series of interstitial-oxygen ordered phases with discrete oxygen contents of  $\text{La}_2\text{NiO}_{4+(1/2n)}$  ( $n=2,3,4,\dots$ ).<sup>12</sup>

Concerning the  $\sqrt{2}a \times p\sqrt{2}a \times qc$ -type superstructure, the excess oxygen atoms are separated from each other by  $\sqrt{2}a$  along the  $[1\bar{1}0]$  direction and by  $p\sqrt{2}a$  along the  $[110]$  direction within a basal plane as shown in Fig. 5. For  $p=2$  the  $[1\bar{1}0]$  excess oxygen rows are shifted by  $\sqrt{2}a$  along the  $[110]$  direction in adjacent basal planes to form a body-centered-orthorhombic lattice sized to  $\sqrt{2}a \times 2\sqrt{2}a \times c$  as shown in Fig. 3. For  $p > 2$  a monoclinic superlattice unit cell seems to be formed. Excess oxygen content is again generally expressed as  $\delta=1/2p$ . The alignment of excess oxygen atoms along the  $[1\bar{1}0]$  direction is more similar to that in the Bi compounds than the alignment along  $[100]$  in the former mode.

We encountered experimental difficulties in confirming the relation between these superstructures and excess oxygen content. Various superstructures appeared or disappeared as they were illuminated by the electron beam even in the normal observation mode. The  $2a \times ka \times lc$  type structure tended to reduce its  $n$  value on irradiation, for example from  $n=4$  to  $n=2$ , while the incommensurate  $\sqrt{2}a \times p\sqrt{2}a \times qc$  mode with  $2 < p < 3$  changed to the commensurate mode with  $n=2$ . It also happened that superlattice spots, once disappeared on heating for a few seconds by the electron beam intensified by removing the condenser aperture, reappeared just as before in a few tens of seconds as continuously monitored using the aperture again. We have interpreted these results as indicating that excess oxygen atoms are rather mobile and become localized in an ordered way only at low temperatures, not much higher than room temperature. This point should be considered in preparing single ordered phases.

Our XRD studies of the present samples indicated a wide monophasic range, though the unit cell varied with  $\delta$  as orthorhombic ( $a_o \sim b_o \sim \sqrt{2}a$  and  $c_o \sim c$ ) for  $\delta \sim 0.0$ , tetragonal ( $\text{K}_2\text{NiF}_4$  type) for  $0.04 \leq \delta \leq 0.12$ , and mono-

clinic ( $a_m \sim b_m \sim a$ ,  $c_m \sim c$ , and  $\gamma \sim 90^\circ$ ) for  $\delta \sim 0.20$ : This is inconsistent with the phase separation reported by Jorgensen *et al.*<sup>2</sup> Probably these diffraction studies observed incompletely ordered or completely disordered states. We are now carefully annealing samples at low

temperatures to obtain ordered serial phases of  $\text{La}_2\text{NiO}_{4+\delta}$  with  $\delta = 0, \dots, \frac{1}{6}, \frac{1}{4}$ .

The present results concerning the  $M = \text{Ni}$  system shed light on the  $M = \text{Co}$  and  $\text{Cu}$  systems, too. The  $\text{La}_2\text{CuO}_{4+\delta}$  system is now under investigation.

<sup>1</sup>J. D. Jorgensen, B. Dabrowski, Shiyu Pei, D. G. Hinks, and L. Soderholm, *Phys. Rev. B* **38**, 11 337 (1988).

<sup>2</sup>J. D. Jorgensen, B. Dabrowski, Shiyu Pei, D. R. Richards, and D. G. Hinks, *Phys. Rev. B* **40**, 2187 (1989).

<sup>3</sup>C. Chailout, S. W. Cheong, Z. Fisk, M. S. Lehmann, M. Marezio, B. Morosin, and J. E. Schirber, *Phys. Scr.* **T29**, 97 (1989).

<sup>4</sup>B. Dabrowski, J. D. Jorgensen, D. G. Hinks, S. Pei, D. R. Richards, H. B. Vanfleet, and D. L. Decker, *Physica C* **162-164**, 99 (1989).

<sup>5</sup>B. Dabrowski, J. D. Jorgensen, D. G. Hinks, Shiyu Pei, D. R. Richards, K. G. Vandervoort, G. W. Crabtree, H. B. Vanfleet, and D. L. Decker (unpublished)

<sup>6</sup>For example, M. Takano, T. Okita, N. Nakayama, Y. Bando,

Y. Takeda, O. Yamamoto, and J. B. Goodenough, *J. Solid State Chem.* **73**, 140 (1988).

<sup>7</sup>E. A. Hewat, J. J. Capponi, and M. Marezio, *Physica C* **157**, 502 (1989).

<sup>8</sup>Y. Le Page, W. R. MacKinnon, J.-M. Tarascon, and P. Barboux, *Phys. Rev. B* **40**, 6810 (1989).

<sup>9</sup>H. W. Zandbergen, W. A. Groen, F. C. Mijlhoff, G. van Tendeloo, and S. Amelinckx, *Physica C* **156**, 325 (1988).

<sup>10</sup>Y. Ikeda, Z. Hiroi, H. Ito, S. Shimomura, M. Takano, and Y. Bando, *Physica C* **165**, 189 (1990).

<sup>11</sup>Y. Matsui, H. Maeda, Y. Tanaka, and S. Horiuchi, *Jpn. J. Appl. Phys. Pt. 2* **27**, L361 (1988).

<sup>12</sup>Z. Hiroi *et al.* (unpublished).

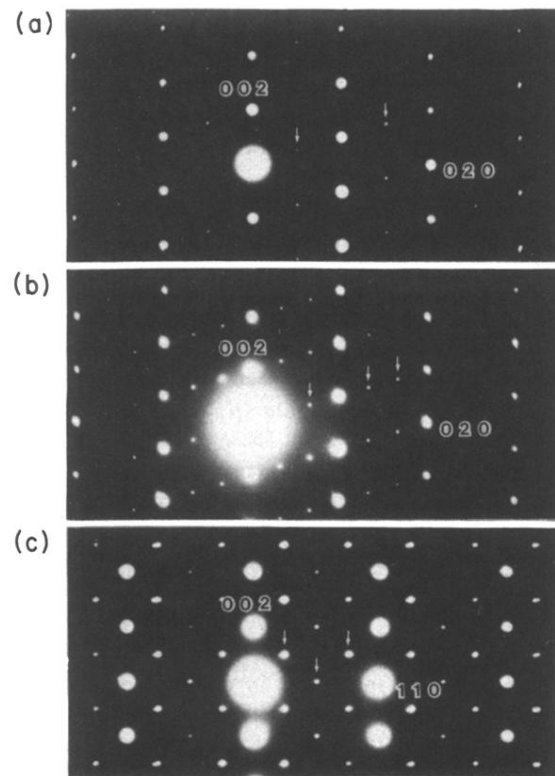


FIG. 1. [100] zone axis ED patterns of the  $2a \times ka \times lc$ -type superstructures with (a)  $k/2=l/2=n=2$ , (b)  $k=l/2=n=3$ , and (c) the  $[1\bar{1}0]$  ED pattern from the  $\sqrt{2}a \times 2\sqrt{2}a \times c$  structure. Certain superlattice reflection spots are marked by arrows.

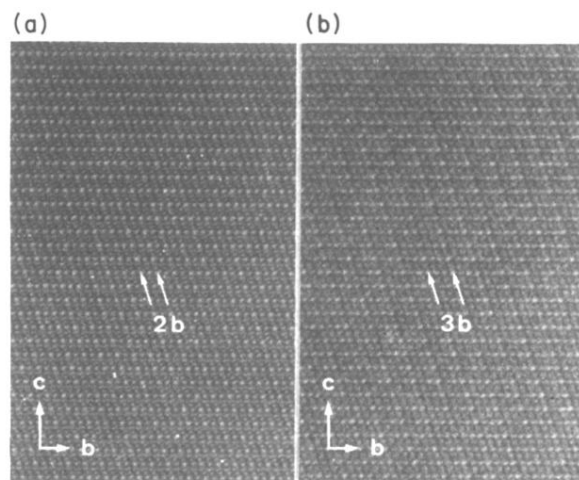


FIG. 2. Lattice images of the  $2a \times ka \times lc$ -type superstructures for (a)  $k/2 = l/2 = n = 2$  and (b)  $k = l/2 = n = 3$  corresponding to the ED patterns in Figs. 1(a) and 1(b), respectively. The brighter (011) lattice fringes are periodically seen as shown by arrows.

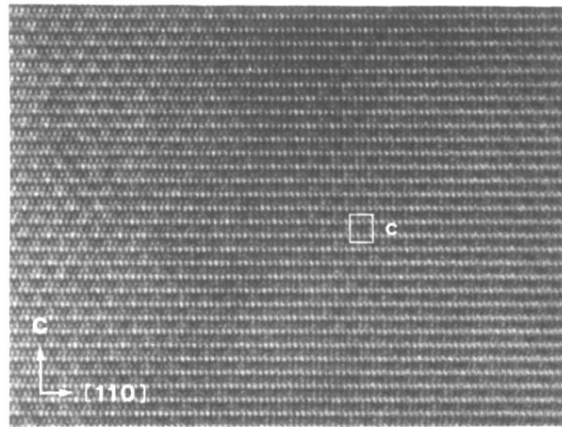


FIG. 3. Lattice images of the  $\sqrt{2}a \times 2\sqrt{2}a \times c$ -type superstructures corresponding to the ED pattern of Fig. 1(c). The fine contrast variation within the LaO layers due to the superlattice is clearly seen, which resembles that of the modulation found in the Bi compounds.